Association of NR3A with the *N*-Methyl-D-aspartate Receptor NR1 and NR2 Subunits

RANA A. AL-HALLAQ, BRYAN R. JARABEK, ZHANYAN FU, STEFANO VICINI, BARRY B. WOLFE, and ROBERT P. YASUDA

Departments of Pharmacology (R.A.A., B.R.J., B.B.W., R.P.Y.) and Physiology (Z.F., S.V.), Interdisciplinary Program in Neuroscience (R.A.A., S.V., B.B.W., R.P.Y.), Georgetown University Medical Center, Washington DC

This article is available online at http://molpharm.aspetjournals.org

ABSTRACT

The NR3A subunit of the *N*-methyl-D-aspartate receptor has been shown to form glutamatergic receptor complexes with NR1 and NR2 subunits and excitatory glycinergic receptor complexes with NR1 alone. We developed an antibody to NR3A and, using quantitative immunoblotting techniques, determined the degree of association between the NR3A subunit and the NR1 and NR2 subunits as well as changes in these associations during development. NR3A expression peaks between postnatal days 7 and 10 in the cortex, midbrain, and hippocampus and reaches higher maximal expression levels in these areas than in the olfactory bulb and cerebellum. Immunoprecipitation experiments with an anti-NR1 antibody demonstrated that the majority of NR3A is associated with NR1 in postnatal day 10 rat cortex (80 $\pm$ 8%), decreasing by half (38 $\pm$ 4%) in the adult rat cortex. Using the anti-NR3A antibody in immunoprecipitation studies, we find that 9.7 $\pm$ 0.8% of NR1, 8.7 $\pm$ 1.8% of NR2A, and 5.0 $\pm$ 0.6% of NR2B are associated with NR3A at postnatal day 10. These values decrease by about half in adult rat cortex. The results of this study demonstrate that NR3A is expressed, distributed, and associated with other subunits in a manner that supports its role in synaptic transmission throughout the rat brain, perhaps playing different roles during development.

The glutamate receptor family mediates the majority of fast excitatory synaptic transmission in the mammalian central nervous system. The ionotropic glutamate receptors are divided pharmacologically into three major groups: the *N*-methyl-D-aspartate (NMDA) receptor (NMDAR), the α-amino-3-hydroxy-5-methyl-4-isoxazolepropionic acid receptor, and the kainate receptor. The NMDAR has received much attention because of its involvement in neuronal development, a variety of neurodegenerative diseases, and certain types of excitotoxicity (Dingledine et al., 1999; Cull-Candy et al., 2001). A voltage-dependent magnesium block and relatively high calcium permeability have implicated the NMDAR in a mechanism thought to be critical for certain types of learning and memory, namely long-term potentiation (McBain and Mayer, 1994).

The NMDAR complex is a tetrameric or pentameric structure composed of at least two NR1 subunits and two or three subunits from the NR2 family (NR2A–D) (for review, see McBain and Mayer, 1994; Dingledine et al., 1999). The NR1

subunit is expressed throughout the central nervous system and is required for the formation of functional receptors. Three alternatively spliced cassettes (for review, see Zukin and Bennett, 1995) in NR1 determine various properties of the ion channel (Dingledine et al., 1999) and are spatio-temporally regulated (Laurie and Seeburg, 1994; Zhong et al., 1995; Prybylowski and Wolfe, 2000). Similarly, each NR2 subunit confers upon the receptor different functional properties (Monyer et al., 1992), and its proper expression is regulated temporally and spatially (Watanabe et al., 1992; Ishii et al., 1993; Monyer et al., 1994; Dunah et al., 1996). The role of the more recently identified NR3 family of subunits (NR3A and NR3B) (Ciabarra et al., 1995; Sucher et al., 1995; Sun et al., 1998; Hayashi et al., 2000; Chatterton et al., 2002; Matsuda et al., 2002) has yet to be clearly determined. Two functions have been identified: first, incorporation of an NR3 subunit into NR1/NR2 receptor complexes results in an NMDAR of decreased functionality (Ciabarra et al., 1995; Sucher et al., 1995; Das et al., 1998; Pérez-Otaño et al., 2001); second, an NR1/NR3 excitatory glycinergic receptor channel has more recently been identified (Chatterton et al., 2002).

Regulation of the expression of the various NMDAR subunits is critical in forming a receptor channel with the desired properties. Messenger RNA studies on NR3A (previous-

ABBREVIATIONS: NMDA, *N*-methyl-D-aspartate; NMDAR, *N*-methyl-D-aspartate receptor; KLH, keyhole limpet hemocyanin; P*x*, postnatal day *x*; HEK, human embryonic kidney; TFEE, Tris-HCl/NaF/EDTA/EGTA; DOC, deoxycholate.

ly named χ-1 or NMDAR-L) and NR3B also report spatial and temporal regulation (Ciabarra et al., 1995; Sucher et al., 1995; Goebel and Poosch, 1999**;** Sun et al., 2000; Nishi et al., 2001; Chatterton et al., 2002). Furthermore, a long splice variant form of NR3A has been identified (NR3A-l), exhibiting an overlapping but unique mRNA expression pattern relative to the short splice variant form (NR3A-s) (Sun et al., 1998).

Reports that the NR3A subunit is enriched at the postsynaptic density and coimmunoprecipitates with NR1 and NR2B (Das et al., 1998) suggest a role for the subunit at the synapse. Direct evidence for a role in synaptic transmission in vivo comes from NR3A knock-out mice in which the NMDA-induced current density in cerebrocortical cells was found to be 2.8-fold greater than in wild-type cells (Das et al., 1998). Furthermore, the cells were morphologically altered and had a greater number of dendritic spines. These findings are supported by functional studies in *Xenopus laevis* oocytes reporting a decrease in the current amplitude when NR3A is cotransfected with NR1, or NR1 and NR2B or NR2D (Ciabarra et al., 1995; Sucher et al., 1995). Moreover, single-channel recordings in *X. laevis* oocytes and human embryonic kidney (HEK) 293T cells reported a smaller unitary conductance, altered mean open time, and 5-fold lower calcium permeability when NR1 and NR2A are coexpressed with NR3A (Das et al., 1998; Pérez-Otaño et al., 2001; Chatterton et al., 2002). Finally, cotransfection of NR3B, which is restricted to motor neurons of the spinal cord and the brainstem (Nishi et al., 2001; Chatterton et al., 2002), with NR2A and NR1 altered the magnesium sensitivity of the NMDAR (Chatterton et al., 2002).

The NR3A and NR3B subunits act as dominant negative regulators of the NMDAR current and have been shown to alter the two most prominent properties of the NMDAR: calcium permeability and magnesium sensitivity. Although this suggests that NR3A may play an important regulatory role, much work remains to be done on the function of the subunit in vivo. We developed an antibody to NR3A and set out to determine the association of NR3A with the other NMDA receptor subunits as well as the regional and developmental expression of NR3A in rat brain. To begin to investigate the role of NR3A, immunoprecipitation experiments were conducted to determine the levels of NR3A associated with other NMDAR subunits from P10 and adult rat cortex and, importantly, the amounts of NR1 and NR2 associated with NR3A.

Materials and Methods

Antibody Production and Affinity Purification. An antibody against the peptide CSRKTELEEYQKTNR was made based on the report by Ciabarra and Sevarino (1997). This peptide corresponds to the amino acids 1098 to 1111 (sequence 17 to 4 amino acids upstream of the carboxyl terminus of NR3A). The peptide, coupled to keyhole limpet hemocyanin (KLH), was synthesized by Research Genetics (Huntsville, NJ). Two rabbits were immunized by Lampire Biologicals (Pipersville, PA) subcutaneously with 0.2 mg of KLH-peptide conjugate in Complete Freund's adjuvant and boosted 1 and 2 weeks later with 0.2 mg of KLH-peptide conjugate in Incomplete Freund's adjuvant. This was followed by the first test bleed 2 weeks later. After this time, immunizations and production bleeds were alternated every 2 weeks.

Affinity columns for NR3A-specific antiserum purification were

prepared by coupling the reduced (by Reduce-Imm Reducing Kit; Pierce, Rockford, IL) peptide to SulfoLink (Pierce) according to the manufacturer's instructions. Antiserum to NR3A was incubated with the affinity resin overnight at 4°C with constant rotation. The resin was washed with 30 bed volumes of binding buffer (100 mM boric acid, 200 mM NaCl, 0.02% sodium azide, pH 8), which was used for all subsequent washes. The bound antibody was eluted with 10 bed volumes of ImmunoPure Gentle Ag/Ab elution buffer (pH 6.9; Pierce), and the resin was washed with 10 bed volumes of binding buffer. A second elution was performed using the ImmunoPure IgG elution buffer (Pierce), followed by a final 30-bed-volume wash of the resin with binding buffer. The eluates were concentrated using Centricon Plus 20 concentrators (Millipore, Bedford, MA) and stored at 4°C in binding buffer. Antibody titer seemed stable for at least 12 months. Approximately 100 μg of antibody was purified from each milliliter of original antiserum as determined by Coomassie blue staining of 10% polyacrylamide gels after SDS polyacrylamide gel electrophoresis, using bovine serum albumin as a standard.

Purification of Total RNA. Rat occipital cortex, midbrain, and olfactory bulb were harvested from rats on P7. For every 100 μg of tissue, 1 ml of TRIzol (Invitrogen, Carlsbad, CA) was added. The tubes were incubated at 30°C for 1 min, vortexed, and incubated at 30°C for 5 min. Chloroform was added at 200 μl per 1 ml of TRIzol and shaken vigorously by hand for 15 s. The solution was incubated at room temperature for 3 min and centrifuged at 7800g_{max} in a Sorvall microcentrifuge for 15 min at 4°C. The aqueous phase was transferred to a fresh tube, and 500 μl of isopropyl alcohol was added (per 1 ml of original TRIzol). The solution was mixed and centrifuged at 7800g_{max} for 10 min at 4°C. The supernatant was discarded, and 1 ml of 75% ethanol (per milliliter of original TRIzol) was added. The sample was centrifuged at 3800g_{max} for 5 min at 4°C, the supernatant was discarded, and the tube was inverted continuously for 10 min. The RNA was then resuspended in DEPC-treated water, and the RNA concentration was determined based on the absorbance at 260 nm.

Production of NR3A Long Construct. Primers corresponding to bases 2829 to 2845 (CATCATCCTTCTCAAGG) and 3804 to 3822 (AAAGGGCCCTAGGAATTCACAAGTCCG) (GenBank accession number AF073379) and containing *Eco*NI and *Apa*I sites, respectively, were synthesized by Invitrogen. The RNA samples purified from rat brain were reverse transcribed and the cDNA amplified using a SuperScript II kit (Invitrogen) according to the manufacturer's instructions. Thirty cycles were set at 94°C for 15 s, 55°C for 15 s, and 72°C for 2 min, with a final 72°C incubation for 10 min, followed by a 4°C incubation overnight. Both the PCR product and the NR3A short construct were digested using *Eco*NI and *Apa*I and separated on a 1.2% agarose gel. The appropriate bands were excised, purified by the gel extraction kit (QIAGEN, Valencia, CA), ligated using T4 DNA Ligase, and transformed into DH5α competent cells (Invitrogen). The construct was purified using the QIAPrep Miniprep Kit (QIAGEN) and digested with *Sap*I to confirm the presence of the insert. The DNA was then sequenced for verification.

Cell Transfection and Crude Membrane Preparation. Dishes (100 mm) of HEK293 cells (Invitrogen) were transfected and harvested as described previously(Al-Hallaq et al., 2001). Protein concentrations were determined using the bicinchoninic acid method (Pierce). The NR1$_{011}$ and NR2A cDNAs were a gift of Dr. S. Nakanishi (Kyoto University, Japan) and were ligated into pcDNA I/AMP, as described previously (Wang et al., 1995). NR2B pRK5 was a gift of Dr. R. Huganir (Johns Hopkins University, Baltimore, MD). NR2C was a gift of Dr. S. Heinemann (Salk Institute, La Jolla, CA) and was ligated into pcDNA I/Amp. NR2D pCDM8 was a gift of Dr. P. Seeburg (Max-Planck Institute, Heidelberg, Germany). NR3A pBK was a gift of Dr. S. Lipton (Burnam Institute, La Jolla, CA). HA-NR3B pTrace was a gift from Dr. M. Yuzaki (St. Jude Children's Research Hospital, Memphis, TN). This NR3B construct is tagged with a hemagglutinin epitope at the carboxyl terminus. Fyn kinase (fyn)

pBK was a gift of Dr. S. Swope (Georgetown University Medical Center, Washington, DC).

Rat brain tissue was harvested from rats on postnatal days 2, 4, 7, 11, 16, 22, 28, 35, and 42, homogenized in ice-cold TFEE buffer (10 mM Tris-HCl, 5 mM NaF, 1 mM EDTA, 1 mM EGTA, pH 7.4), centrifuged at $30,000g_{max}$ for 10 min at 4°C. The pellet was resuspended in ice-cold TFEE buffer and stored at -70°C. For immunoblots, samples were thawed for 2 min in a 37°C water bath and sonicated. One volume of $4\times$ treatment buffer (0.25 M Tris-HCl, pH 6.8, 8% SDS, 200 mM dithiothreitol, 30% glycerol) was added to three volumes of sample, and the resulting samples were placed in a boiling water bath for 5 min and divided into aliquots for immunoblotting.

Coupling of Antibodies to Protein A Sepharose Beads. Protein A Sepharose CL-4B beads (Sigma, St. Louis, MO) were washed three times in 1 ml of 0.2 M sodium borate, pH 8.0. Beads were then incubated with antibodies to either anti-NR1 (Luo et al., 1997) or anti-NR3A in a 1:2 ratio of micrograms of antibody to microliters of beads at room temperature for 1 h with constant rotation, followed by three washes in 1 ml of immunoprecipitation buffer (0.1% Triton X-100 and 50 mM Tris-HCl, pH 7.4) and centrifugation between each wash at $7800g_{max}$ for 15 s.

Solubilization and Immunoprecipitation. Membrane fractions from transfected HEK293 cells, P10 cortex, or adult cortex were diluted in TFEE buffer to 1 mg of total protein per milliliter. For every 100 μl of membrane preparation, 10 μl of deoxycholate (DOC) stock (10% DOC, 500 mM Tris-HCl, pH 9) was added, and the solution was incubated at 37°C for 30 min with regular mixing by inversion. After incubation, 10 μl of solution (containing 1% Triton X-100, 500 mM Tris-HCl, pH 9, and 1% DOC) was added for each 100 μl of original sample, and the solution was centrifuged at $30,000g_{max}$ for 30 min. For each reaction, 20 μl of washed protein A Sepharose beads coupled to anti-NR1 or anti-NR3A antibody (see above) in 102 μl of immunoprecipitation buffer (0.1% Triton X-100 and 50 mM Tris-HCl, pH 7.4) was added to 48 μl (40 μg) of solubilized protein to a final volume of 150 μl. After this incubation with constant rotation at 4°C for 2 h, samples were centrifuged at $7800g_{max}$ for 15 s, the supernatant (150 μl) was removed and added to 50 μl of $4\times$ treatment buffer. The pellets were washed three times in 1 ml of immunoprecipitation buffer, and the beads were brought up in 75 μl of immunoprecipitation buffer and 25 μl of $4\times$ treatment buffer and boiled. Supernatant and pellet samples were loaded onto 7.5% SDS-polyacrylamide gels and subjected to electrophoresis.

Immunoblotting. Immunoblotting was carried out as described previously (Al-Hallaq et al., 2001) with the following modifications. Standard curves using membranes prepared either from HEK293 cells transfected with NR3A cDNA or adult rat cortex were loaded at 1.6-fold dilutions. Immunoblots were probed with anti-NR3A or with Pan NR1, NR2A, and NR2B antibodies, which have been previously characterized in this laboratory (Wang et al., 1995; Luo et al., 1997). To recognize the HA-NR3B, the anti-hemagglutinin mouse monoclonal antibody, 12CA5, was purchased from Roche Molecular Biochemicals (Indianapolis, IN). SuperSignal West pico chemiluminescent and West femto maximum sensitivity substrates were obtained from Pierce.

Peptide Blockade of the NR3A Antibody. The CSRK-TELEEYQKTNR and CRVEKRSNLGPQQ peptide affinity resins were used to demonstrate the specificity of the NR3A antibody. Ten micrograms of the affinity-purified NR3A antibody in 350 μl of binding buffer and 150 μl of either the CSRKTELEEYQKTNR or the CRVEKRSNLGPQQ peptide affinity resin were incubated at 22°C with rotation (30 rpm) for 2 h in a microcentrifuge tube. Each tube was centrifuged for 15 s at $\sim$8000g and the supernatant was transferred to another tube. The resin pellets were washed $2\times$ with 325 μl of Tris-buffered saline/Tween 20 (50 mM Tris-HCl, pH 7.6, 137 mM NaCl, and 0.1% Tween 20). The washes were pooled with the initial supernatant for each peptide affinity resin. Two hundred and fifty microliters of each was added to 25 ml of Tris-buffered saline/Tween

20 with 5% nonfat dried milk to make a antibody concentration of about 1 μg/ml if no antibody bound to the peptide affinity resin.

Results

Anti-NR3A Specifically Recognizes NR3A. An antibody was raised to a peptide sequence four amino acids upstream of the carboxyl terminus of NR3A. HEK293, P7 cortex, and P7 thalamus membrane fractions were used to test the specificity of the NR3A antibody. Lanes 5 to 16 of Fig. 1 show an immunoblot probed with the affinity-purified anti-NR3A antibody at 1 μg/ml and developed with the SuperSignal West pico chemiluminescent substrate. A band was detected at the size expected for the glycosylated form of NR3A (135 kDa) (Ciabarra and Sevarino, 1997) only in those lanes containing HEK293 cells transfected with the short (NR3A-s) or long (NR3A-l) splice variant form cDNA. Cells transfected with an unrelated protein, fyn kinase, or the NMDAR NR1 or NR2 cDNA show no signal at the expected molecular mass. This was true even when the more sensitive SuperSignal West femto was used (data not shown). Parallel immunoblots were probed with antibodies to NR1, NR2A, NR2B, and fyn kinase to verify the expression of these subunits (data not shown). Membrane fractions from P7 thalamus (lane 15) and cortex (lane 16) were immunopositive at 135 kDa, as expected from previous studies (Ciabarra and Sevarino, 1997). The molecular mass of NR3A does not seem to differ in HEK293 cells and in P7 brain, suggesting that NR3A is glycosylated in HEK293 cells, as reported previously (Ciabarra and Sevarino, 1997).

Lanes 3 and 4 are loaded with 20 μg of HEK293 cells transfected with NR1/HA-NR3B. lane 3 is immunoblotted with an anti-hemagglutinin mouse monoclonal antibody to demonstrate the presence of NR3B that has been tagged on the carboxyl terminus with hemagglutinin (Matsuda et al., 2002). The hemagglutinin antibody has a nonspecific band at about 150 kDa that is present in all HEK293 cells whether or not the cells have been transfected with any of the NMDA receptor subunits. Only HEK293 cells that were transfected with NR3B demonstrated an immunoreactive band at around 116 kDa identical to that recently reported by Matsuda et al. (2002). When 20 μg of protein from a parallel blot loaded with the HEK293 cells transfected with NR1/HA-NR3B is was probed with the NR3A antibody, no immunoband at 116 kDa was detected even when SuperSignal West femto is used (lane 4).

Figure 1, lane 1, demonstrates the ability of the immunizing peptide to block the specific immunoreactivity of the anti-NR3A peptide; lane 2 demonstrates that an unrelated peptide had no effect. For this experiment, NR3A antibodies were preincubated with either the CSRKTELEEYQKTNR or the CRVEKRSNLGPQQ peptide affinity resin. The CSRK-TELEEYQKTNR peptide was used to immunize the rabbits producing the NR3A antibodies. The supernatant from this affinity resin was unable to generate immunoreactive bands on an immunoblot (lane 1). There is no evidence of any bands even though SuperSignal West femto was used. However, when the NR3A antibodies were preincubated with a CRVEKRSNLGPQQ peptide affinity resin, the supernatant from this affinity resin generated immunoreactive band on an immunoblot (lane 2). This lane was also developed with SuperSignal West femto.
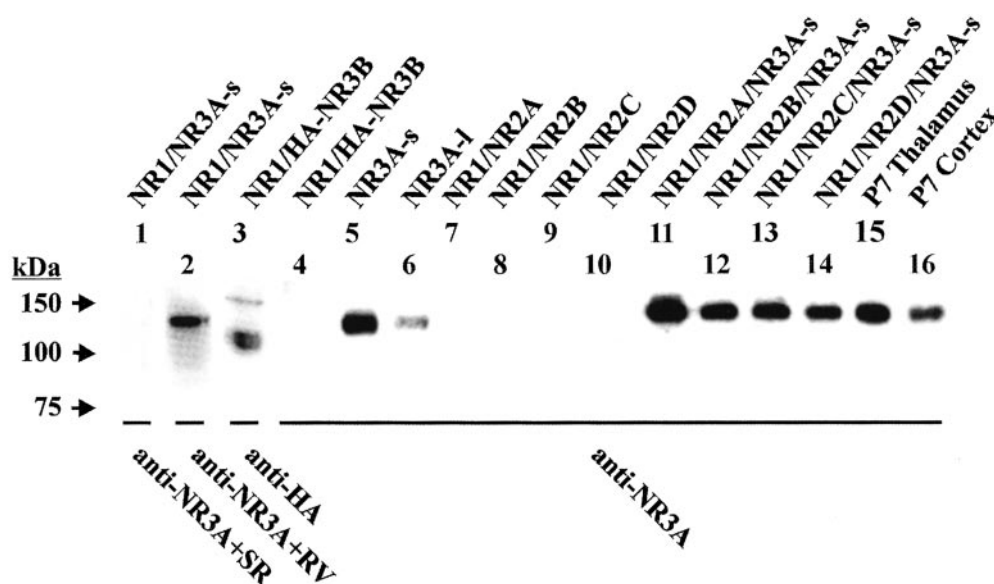
Fig. 1. The anti-NR3A antibody is specific for NR3A. When probed with the NR3A antibody (1 μg/ml), HEK293 cells transfected with cDNA of NR3B C-terminally tagged with hemagglutinin (HA-NR3B; lane 4), or with NR1, NR2A, NR2B, NR2C, or NR2D (lanes 7–10, respectively) show no cross-reactivity with NR3A. HEK293 cells transfected with the short (NR3A-s; lane 5) or long (NR3A-l; lane 6) splice variant form of NR3A alone, or with NR1 and NR2A, NR2B, NR2C, or NR2D (lanes 11–14, respectively) are immunopositive for NR3A. Lanes 3 and 4 were loaded with 20 μg/lane of transfected HEK293 cells. Lanes 1 and 2 were loaded with 5 μg/lane of transfected HEK293 cells. Lanes 5–16 were loaded with transfected HEK293 cells at 1 μg per lane. P7 thalamus and cortex are immunopositive for NR3A (5 μg per lane). The NR3A-s transfected HEK293 cells were tested against NR3A antibodies that were preincubated with the CSRKTELEEYQKTNR peptide (SR) used to make the antiserum (lane 1) or an unrelated peptide (RV; lane 2). Lanes 1 to 4 were developed with the SuperSignal West femto and lanes 5 to 16 were developed with SuperSignal West pico.
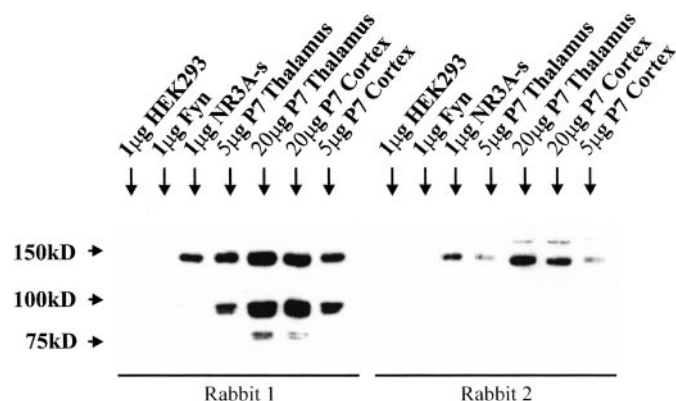
Affinity-purified antibodies from both immunized rabbits generated a specific band at 135 kDa when the blots were developed with SuperSignal West pico. When the immunoblots were developed with the highly sensitive SuperSignal West femto substrate, nonspecific bands were detected in the rat cortex and thalamus (Fig. 2) in addition to the immunopositive band at 135 kDa. Antibodies from the two rabbits exhibited differing patterns of nonspecific bands, confirming that these bands are nonspecific and are not breakdown products. When antibodies from one of the two rabbits were tested, no signal was detected in untransfected or fyn kinase

Fig. 2. Immunoblots tested against affinity-purified antibodies from two rabbits immunized with the NR3A antigen show immunoreactive bands around 135 kDa and nonspecific bands of other sizes when blots are developed using SuperSignal West femto reagents. Immunpositive bands of the expected size are seen only in HEK293 cells transfected with NR3A-s or with P7 thalamus and cortex using affinity purified antibodies from either rabbit. Total protein load is indicated. The variation in nonspecific band patterns from the affinity-purified antibodies from the two rabbits demonstrates that all bands other than those at 135 kDa are nonspecific and are not caused by proteolysis of the NR3A protein.

transfected HEK293 membrane fractions even with this highly sensitive developing reagent.

Developmental and Regional Expression of NR3A. To determine the spatial and temporal expression patterns of NR3A, a series of immunoblotting experiments with membrane fractions from various rat brain regions at varying ages was carried out. The signal was quantified relative to a standard curve in which membranes from HEK293 cells transfected with NR3A-s were loaded at 1.6-fold dilutions as described previously by Wang et al. (1995).

In cortex, hippocampus, and midbrain (Fig. 3, A, B, and C, respectively), NR3A was relatively high at P2, the earliest time point studied, and increased to peak levels between P7 and P10. Protein levels in the three brain regions declined after this time point and reached near steady-state levels by P30 but remained detectable even at P42 (the oldest time point examined). In contrast, in the cerebellum (Fig. 3D), levels of NR3A were highest at P2 and declined thereafter until reaching adult levels by P10. In the olfactory bulb (Fig. 3E), NR3A protein levels reached a peak around P5 and declined to low, but detectable, levels in the adult. At P7, the protein levels of NR3A in the cerebellum and olfactory bulb were approximately 25% of those seen in the cortex, midbrain, and hippocampus. This ratio was maintained between the cerebellum and olfactory bulb and the midbrain and hippocampus into adulthood. At P42, the cerebellum had the lowest protein levels of the regions examined. All of these immunoblots were done with SuperSignal West pico.

NR3A Associates with the NR1 Subunit. The assembly of NMDAR subunits into a heteromeric receptor is required for the formation of a functional receptor channel. For NR3A to have a functional effect, it presumably must be associated with other NMDAR subunits. To determine the level of NR3A associated with other NMDAR subunits, we carried out a

series of nondenaturing immunoprecipitation experiments. After membrane fractions were gently solubilized, the protein complex was immunoprecipitated with either antibodies to NR1 or NR3A to determine the level of associated subunits.

P10 and adult cortical membrane preparations were immunoprecipitated using protein A-Sepharose beads noncovalently coupled to anti-NR1 antibody. Although immunoprecipitations with covalently coupled anti-NR1/protein A-Sepharose beads were attempted, a high background signal resulted when the immunoblots were probed with the anti-NR3A antibody. Therefore, the anti-NR1 antibody was noncovalently coupled to protein A-Sepharose beads. How-

ever, the maximum immunoprecipitation efficiency of total NR1 that could be achieved with noncovalently coupled anti-NR1/protein A-Sepharose beads was $60 \pm 2\%$ (mean $\pm$ S.E.M.) in P10 and $70 \pm 1\%$ in adult. In this case, $40 \pm 1\%$ of NR2A, $52 \pm 4\%$ of NR2B, and $48 \pm 4\%$ of NR3A were pulled down with the NR1 subunit in P10 cortex. In the adult cortex, $45 \pm 2\%$ of NR2A, $49 \pm 2\%$ of NR2B, and $26 \pm 3\%$ of NR3A were pulled down with NR1.

To determine the amount of NR2 and NR3A subunits that would have been pulled down with NR1 had the anti-NR1 antibody pulled down all NR1 subunits present in the samples, the NR1 immunoprecipitation efficiency was normalized to 100%. Thus, the percentages of NR2A, NR2B, and
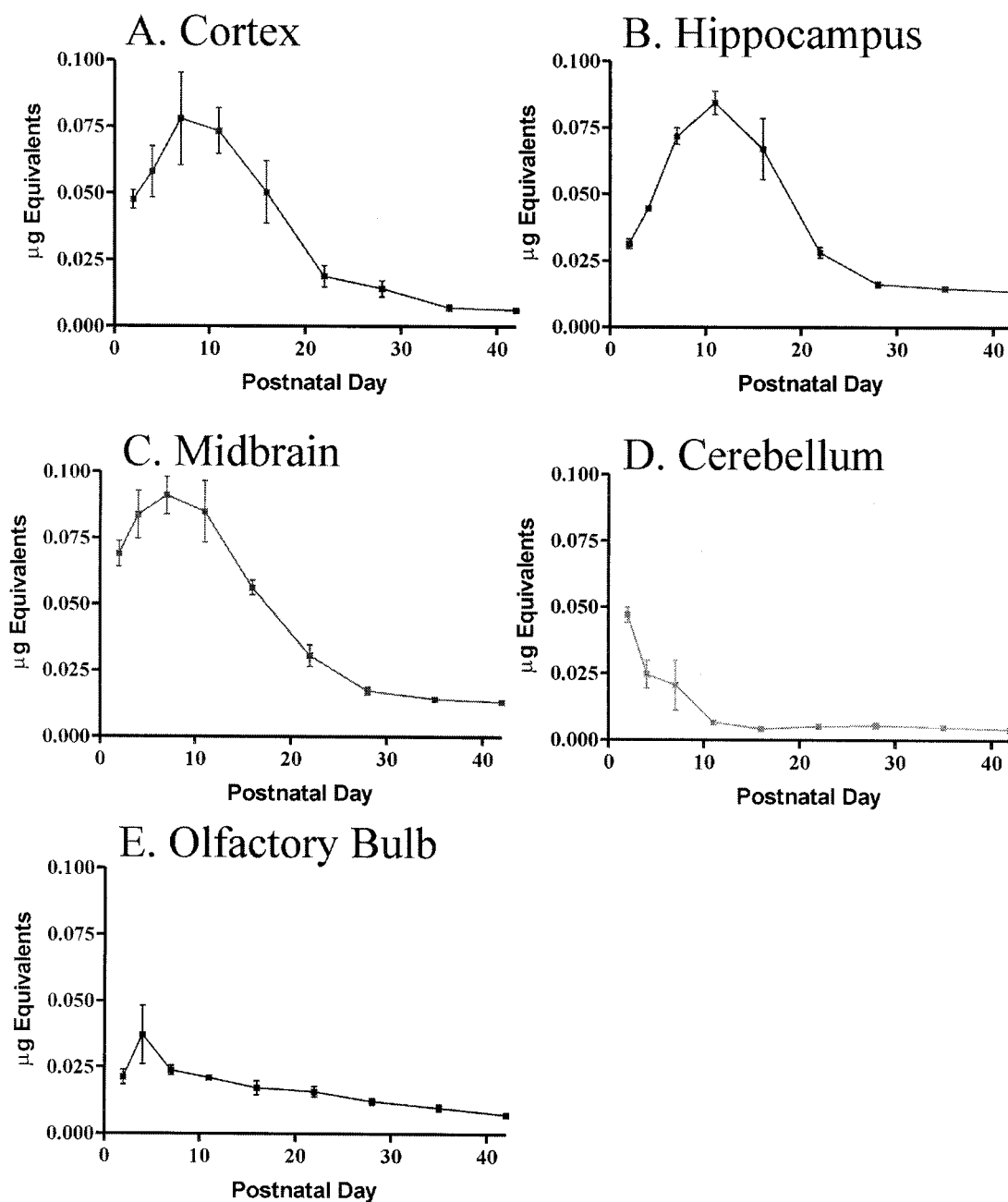
Fig. 3. Expression of the NR3A protein in cortex (A), hippocampus (B), midbrain (C), cerebellum (D), and olfactory bulb (E) from P2 to P42. Immunoblots of these brain regions were performed using the affinity purified anti-NR3A antibody. Levels of NR3A presented as μg equivalents of HEK293 cells transfected with NR3A. Error bars are S.E.M.. All samples were run in duplicate ($n = 5$). These experiments were done using SuperSignal West pico.

NR3A pulled down in these experiments were divided by the fraction of NR1 precipitated in P10 (0.6) or adult (0.7) tissue, resulting in a calculated estimate of the percentage of NR2A, NR2B, or NR3A associated with NR1 in the tissue. P10 cortex (Fig. 4B, ▦) yielded values of 68 ± 4% of NR2A and 88 ± 7% of NR2B associated with NR1. Adult cortex (Fig. 4B, ☐) resulted in corrected values of 65 ± 2% of NR2A and 70 ± 4% of NR2B associated with NR1. These corrected values are similar to our previously reported values of 56 ± 7% of NR2A and 75 ± 5% of NR2B associated with NR1 in experiments in which anti-NR1 was covalently coupled to protein A-Sepharose beads resulting in 100% precipitation of NR1 (Luo et al., 1997). Using these correction factors, we calculate that 80 ± 8% of NR3A in P10 cortex and 38 ± 4% in adult cortex are associated with NR1 (Fig. 4B). A representative immunoblot for NR3A associated with NR1 is shown in Fig. 4A. Controls in which protein A-Sepharose was used without a primary antibody showed no signal in the pellets.

**The Anti-NR3A Antibody Pulls down Other NMDAR Subunits.** Whereas the data presented in Fig. 4 are levels of
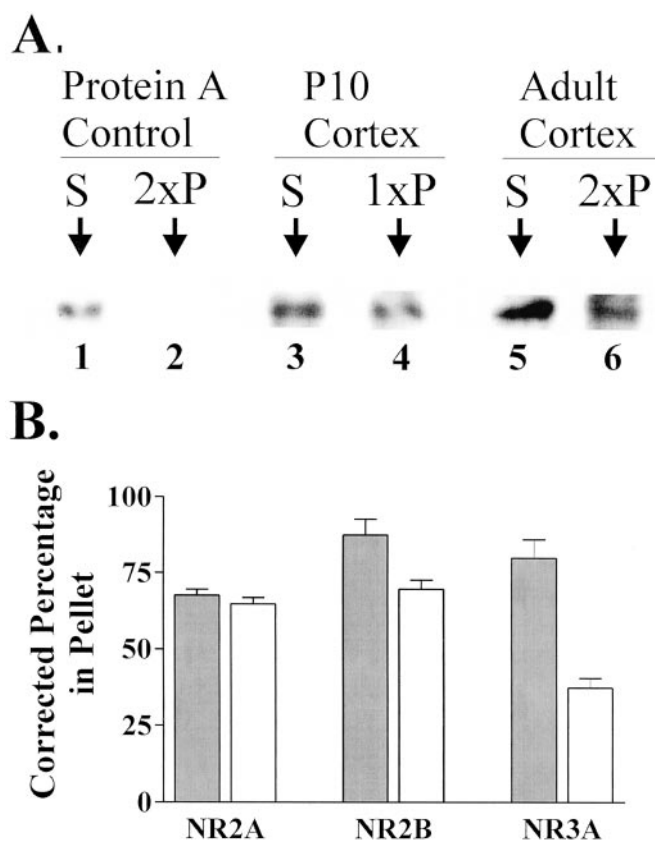
Fig. 4. NR2A, NR2B, and NR3A subunits are associated with NR1 in P10 (▦) and adult (☐) cortical membrane fractions. A, a representative immunoblot of NR3A immunoprecipitations of P10 and adult cortex probed with an anti-NR3A antibody. The supernatant and pellet samples from adult control (protein A; i.e., no anti-NR1, lanes 1 and 2) and anti-NR1 immunoprecipitations from P10 cortex (lanes 3 and 4) and adult cortex (lanes 5 and 6) are shown. When quantified, the amount of protein pulled down nonspecifically in the adult control (lane 2) was subtracted from the total percentage of NR3A immunoprecipitated from the adult cortex pellet. B, native immunoprecipitations with an anti-NR1 antibody were performed. Immunoblots were examined with antibodies against the NR2A, NR2B, and NR3A subunits. Values were quantified relative to a cortical membrane standard and corrected to 100% immunoprecipitation efficiency of NR1 and represented at mean ± S.E.M. All samples were run in duplicate with $n = 4$. In these experiments, SuperSignal West pico was used for NR2A and NR2B. SuperSignal West femto was used for NR3A.

NR2 and NR3A associated with the NR1 subunit, the levels of NR1 and NR2 subunits associated with the NR3A subunit remain to be determined. First, to verify the specificity of the NR3A antibody in immunoprecipitation experiments, we used the antibody to immunoprecipitate solubilized membrane preparations from HEK293 cells transfected with NR1 and NR2 subunits with or without the NR3A subunit (Fig. 5). The SuperSignal West femto was used to detect the signal in the pellets in immunoblots probed with anti-NR3A. In the supernatants, bands for NR3A (as indicated by the arrows) are seen only in those cells transfected with NR3A cDNA (Fig. 5, top left). Nonspecific bands are seen in lanes 1 and 4 (as seen above the arrows). Similarly, in the pellets, NR3A signal is detected only in cells transfected with NR1/NR2A/ NR3A or NR1/NR2B/NR3A (Fig. 5, top right).

NR1 signal is detected in the four lanes loaded with supernatant samples from the anti-NR3A immunoprecipitations (Fig. 5, lanes 1–4). However, NR1 signal is detected only in those pellets in which the cells had been cotransfected with NR3A (Fig. 5, lanes 7 and 8), indicating the anti-NR3A antibody does not nonspecifically pull down NR1. Similar results were seen with NR2A and NR2B, in which signal for the subunits was detected only in the pellet lanes of cells cotransfected with NR3A (Fig. 5, lanes 7 and 8). These experiments suggest that the anti-NR3A antibody specifically immunoprecipitates NR3A and does not nonspecifically bring down NR1, NR2A, or NR2B. Moreover, the NR1, NR2A, and NR2B subunits can each associate with NR3A in HEK293 cells.

Figure 6A shows a representative blot probed with an anti-NR1 antibody from an anti-NR3A immunoprecipitation of P10 and adult cortex. Parallel blots were probed with anti-NR2A and anti-NR2B antibodies; for each antibody, a standard curve of cortical membranes was run at 1.6-fold dilutions for quantification, as described previously(Wang et al., 1995). The tissue concentration, volume of the reaction, and the amount of noncovalently coupled protein A-Sepha-
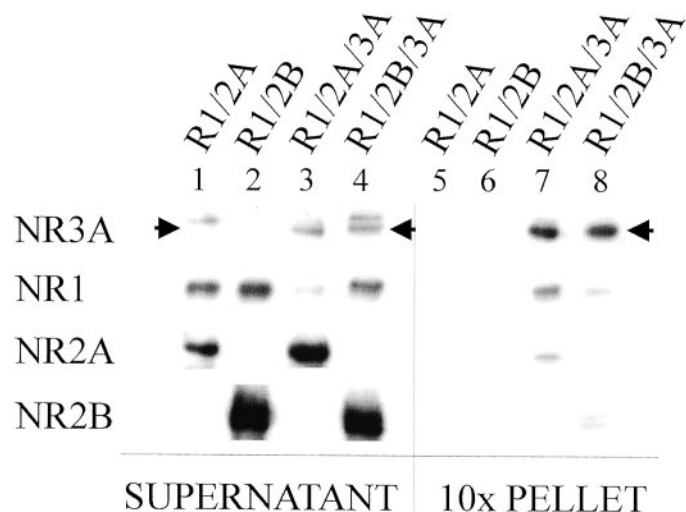
Fig. 5. The anti-NR3A antibody specifically immunoprecipitates NR3A in transfected HEK293 cells. All samples were immunoprecipitated with anti-NR3A antibody. Cells were transfected as indicated across the top, and the immunoblots were probed as indicated on the left. Pellet samples were loaded at 10 times the concentration of supernatant samples. Immunopositive bands are seen in the pellets only in lanes cotransfected with NR3A. The arrows indicate the bands that correspond to NR3A; the bands above the arrows are nonspecific, as seen in Fig. 2, right. These experiments used SuperSignal West femto.

rose/NR3A antibody gave complete immunoprecipitation of NR3A. Under these conditions, the protein A-Sepharose control did nonspecifically pull down a small amount of NR1 in adult, but not P10, cortex, as seen in the protein A control $10\times$ pellet sample (lane 2). When quantified, this value was subtracted from the total percentage of NR1 immunoprecipitated in the adult cortex. Note that supernatant: pellet loads were at a ratio of 1:10 to ensure both supernatant and pellet values were within a similar range of the standard curve for quantification.

In each immunoprecipitation, blots were probed with antibodies to NR1, NR2A, NR2B, and NR3A and quantified (Fig. 6B). In P10 rat cortex, $9.7 \pm 0.8\%$ of NR1, $8.7 \pm 1.8\%$ of NR2A, and $5.0 \pm 0.6\%$ of NR2B were pulled down with NR3A. In the case of adult rat cortex, $3.1 \pm 0.3\%$ of NR1, $2.5 \pm 0.5\%$ of NR2A, and $1.7 \pm 0.5\%$ of NR2B were pulled down. These data demonstrate that although the levels of NR1, NR2A, and NR2B associated with NR3A are higher at P10 than in adult, a small percentage of these subunits are still associated with NR3A in the adult.
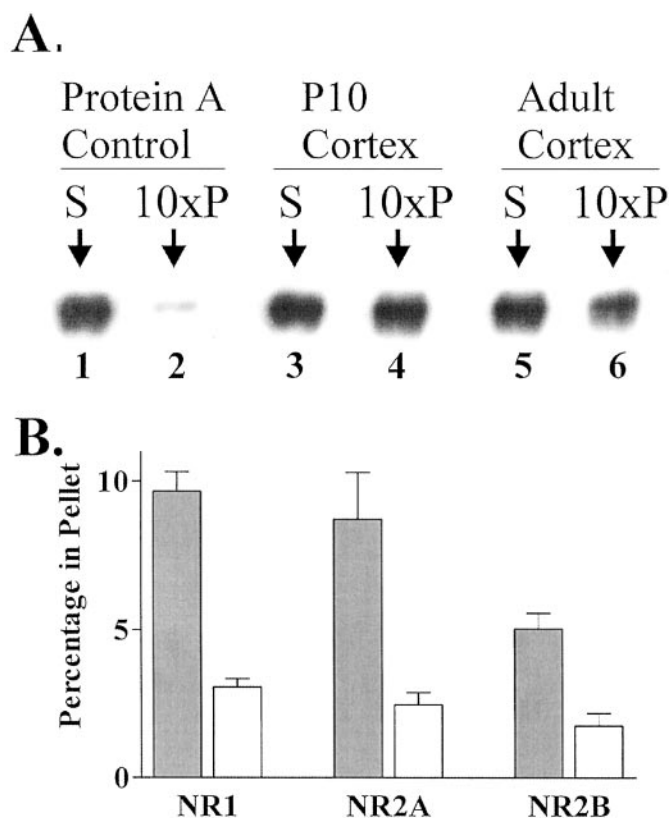
Fig. 6. NR1, NR2A, and NR2B subunits are associated with NR3A in P10 (▦) and adult (□) cortical membrane fractions. A, a representative immunoblot of NR3A immunoprecipitations of P10 and adult cortex probed with an anti-NR1 antibody. The supernatant and pellet ($10\times$ load of supernatants) samples from adult control (no anti-NR3A, lanes 1 and 2) and anti-NR3A immunoprecipitations from P10 cortex (lanes 3 and 4) and adult cortex (lanes 5 and 6) are shown. When quantified, the amount of protein pulled down nonspecifically in the adult control (lane 2) was subtracted from the total percentage of NR1 immunoprecipitated from the adult cortex pellet. B, percentages of the indicated NMDAR subunit were quantified relative to a cortical membrane standard and are represented as mean $\pm$ S.E.M. All samples were run in duplicate with $n = 4$. These experiments used SuperSignal West pico.

Discussion

We have developed a rabbit polyclonal antibody that is specific for the NR3A subunit. In this investigation, it has been used to examine the expression pattern as well as the association of NR3A with the other NMDAR subunits in various brain regions throughout development. We found that expression in the forebrain peaks between P7 and P10, although it is less pronounced and differs temporally in other brain regions. In young animals, the majority of the NR3A subunit was associated with the NR1 subunit, indicating that the subunit is highly coassembled in the receptor complex. Conversely, a smaller fraction of total NR1, NR2A, and NR2B were associated with NR3A.

This polyclonal antibody shows no cross-reactivity with other NR1 or NR2 subunit (Fig. 1, lanes 7–10). Importantly, it also shows no cross-reactivity with the NR3B subunit (Fig. 1, compare lanes 1 and 4), which has 62% homology with the NR3A subunit (Matsuda et al., 2002). Also, the immunizing peptide can block the immunoreactive band at 135 kDa in HEK293 cells transfected with NR3A. However, preincubation of the NR3A antibody with another nonrelated peptide does not affect the presence of the immunoreactive band at 135 kDa. Therefore, this polyclonal antibody seems specific for the NR3A subunit.

Our finding that NR3A protein expression peaks between P7 and P10 in the cortex, midbrain, and hippocampus is consistent with previous reports on NR3A mRNA expression (Ciabarra et al., 1995; Sun et al., 1998). In comparison with the expression patterns of the other NMDAR subunits, NR3A expression most closely resembles that of NR2D in that both subunits peak around P7 (Watanabe et al., 1992; Monyer et al., 1994; Dunah et al., 1996). In contrast, NR1 and NR2A-C increase with developmental age and peak around the third postnatal week (Watanabe et al., 1992; Laurie and Seeburg, 1994; Monyer et al., 1994; Zhong et al., 1995). Significantly, however, whereas NR1, NR2B, and NR2C mRNA can be detected by embryonic day 14 (NR1 and NR2B) or P1 (NR2C) (Watanabe et al., 1992; Monyer et al., 1994), NR2A mRNA is not expressed until around P7 and increases dramatically during the next 2 postnatal weeks (Watanabe et al., 1992; Williams et al., 1993). This increase in expression of NR2A results in a more rapid deactivation of the NMDA-mediated synaptic current because of incorporation of this subunit into synaptic NMDAR (Flint et al., 1997; Kew et al., 1998; Stocca and Vicini, 1998; Rumbaugh and Vicini, 1999; Tovar et al., 2000).

Thus, at P7 to P10, a critical switch in the subunit composition of the NMDAR begins with an up-regulation of the NR2A subunit and a decline in NR3A and NR2D levels. The timing of the peak expression, as well as previous reports demonstrating NR3-containing receptors exhibit a decreased calcium permeability (Das et al., 1998; Pérez-Otaño et al., 2001; Chatterton et al., 2002), suggest that this subunit plays a role in early synaptic rearrangement by causing a decrease in Ca^{+2} entry, similar to the NR2A subunit. The resultant decrease in channel conductance (Ciabarra et al., 1995; Sucher et al., 1995; Das et al., 1998; Pérez-Otaño et al., 2001; Chatterton et al., 2002) and magnesium sensitivity (Chatterton et al., 2002) of NR3-containing NMDAR channels also supports this idea. Analogous to the NR2C- and NR2D-containing receptors, which are implicated in the detection of

low synchronicity in the developing brain because of their resistance to Mg^{+2} blockade relative to NR2A- and NR2B-containing receptors (Monyer et al., 1992, 1994; Ishii et al., 1993), the NR3 subunits may also be involved in synaptic development and maturation.

We found that the maximal expression level of NR3A is higher in the hippocampus, cortex, and midbrain than in the olfactory bulb and cerebellum. The reason for these differences may be that subunit expression in the olfactory bulb and the cerebellum peaks prenatally. Our findings are consistent with those reported by Ciabarra and Sevarino (1997), in which NR3A proteins were shown to be expressed in P7 rat cortex and thalamus. In their study, however, NR3A was not detected in P7 cerebellum or striatum, perhaps because of a higher threshold for detection. Thus, our findings suggest that NR3A may play an important modulatory role throughout the brain.

Importantly, this study quantitates the association of NR3A with other NMDAR subunits. We show that NR3A forms complexes containing NR1 and NR2A or NR2B in rat cortex, as demonstrated previously (Das et al., 1998). The NR3A subunit is highly associated with NR1 at P10 (80 ± 8%), and this association decreases to 38 ± 4% in adult cortex. These immunoprecipitation data suggest that although the majority of NR3A is associated with the NMDAR complex, a small percentage of these complexes contain NR3A. It is possible that the association of NR3A with NR1 in the adult cortex may be weaker than that in P10 cortex and, therefore, more easily disrupted during the solubilization and immunoprecipitation, resulting in lower levels of NR3A being pulled down with NR1 because of experimental factors. The spatial and temporal placement of the NR3A-containing NMDAR complexes may be an important point of regulation at the synaptic level. Furthermore, the temporal change in the amount of NR3A in the NMDAR complex suggests that it plays distinct roles as a negative modulator at the two times in development examined in this study.

A recent study reported that the NR3A and NR3B subunits form excitatory glycinergic receptor channels when associated only with the NR1 subunit (Chatterton et al., 2002). This finding is consistent with a previous study using heterologous systems in which NR1 and NR3A assemblies were shown to reach the plasma membrane even in the absence of an NR2 subunit (Pérez-Otaño et al., 2001); similarly, we were able to show that NR3A coassembles with NR1 in HEK293 cells transfected with only NR1 and NR3A (data not shown).

This article has demonstrated that the association of the NR3A subunit with other NMDAR subunits changed during development. Such changes seemed to be coordinated with other alterations that occured during synaptogenesis, such as the switch in NMDAR subunit composition. Changes in the ability of the NR3A subunit to negatively modulate the NMDAR complex or create a glycine-gated channel may underlie the importance of alterations in NR3A during development. Indeed, the presence of the NR3A subunit could play a pivotal role in whether or not a given synapse meets the necessary threshold to participate in long-lasting changes such as long-term potentiation.

References

Al-Hallaq RA, Yasuda RP, and Wolfe BB (2001) Enrichment of *N*-methyl-D-aspartate NR1 splice variants and synaptic proteins in rat postsynaptic densities. *J Neurochem* **77:**110–119.

Chatterton JE, Awobuluyi M, Premkumar LS, Takahashi H, Talantova M, Shin Y, Cui J, Tu S, Sevarino KA, Nakanishi N, et al. (2002) Excitatory glycine receptors containing the NR3 family of NMDA receptor subunits. *Nature (Lond)* **415:**793–798.

Ciabarra AM and Sevarino KA (1997) An anti-chi-1 antibody recognizes a heavily glycosylated protein in rat brain. *Brain Res Mol Brain Res* **46:**85–90.

Ciabarra AM, Sullivan JM, Gahn LG, Pecht G, Heinemann S, and Sevarino KA (1995) Cloning and characterization of chi-1: a developmentally regulated member of a novel class of the ionotropic glutamate receptor family. *J Neurosci* **15:**6498–6508.

Cull-Candy S, Brickley S, and Farrant M (2001) NMDA receptor subunits: diversity, development and disease. *Curr Opin Neurobiol* **11:**327–335.

Das S, Sasaki YF, Rothe T, Premkumar LS, Takasu M, Crandall JE, Dikkes P, Conner DA, Rayudu PV, Cheung W, et al. (1998) Increased NMDA current and spine density in mice lacking the NMDA receptor subunit NR3A. *Nature (Lond)* **393:**377–381.

Dingledine R, Borges K, Bowie D, and Traynelis SF (1999) The glutamate receptor ion channels. *Pharmacol Rev* **51:**7–61.

Dunah AW, Yasuda RP, Wang YH, Luo J, Davila-Garcia M, Gbadegesin M, Vicini S, and Wolfe BB (1996) Regional and ontogenic expression of the NMDA receptor subunit NR2D protein in rat brain using a subunit-specific antibody. *J Neurochem* **67:**2335–2345.

Flint AC, Maisch US, Weishaupt JH, Kriegstein AR, and Monyer H (1997) NR2A subunit expression shortens NMDA receptor synaptic currents in developing neocortex. *J Neurosci* **17:**2469–2476.

Goebel DJ and Poosch MS (1999) NMDA receptor subunit gene expression in the rat brain: a quantitative analysis of endogenous mRNA levels of NR1Com, NR2A, NR2B, NR2C, NR2D and NR3A. *Brain Res Mol Brain Res* **69:**164–170.

Hayashi Y, Shi SH, Esteban JA, Piccini A, Poncer JC, and Malinow R (2000) Driving AMPA receptors into synapses by LTP and CaMKII: requirement for GluR1 and PDZ domain interaction. *Science (Wash DC)* **287:**2262–2267.

Ishii T, Moriyoshi K, Sugihara H, Sakurada K, Kadotani H, Yokoi M, Akazawa C, Shigemoto R, Mizuno N, Masu M, et al. (1993) Molecular characterization of the family of the *N*-methyl-D-aspartate receptor subunits. *J Biol Chem* **268:**2836–2843.

Kew JN, Richards JG, Mutel V, and Kemp JA (1998) Developmental changes in NMDA receptor glycine affinity and ifenprodil sensitivity reveal three distinct populations of NMDA receptors in individual rat cortical neurons. *J Neurosci* **18:**1935–1943.

Laurie DJ and Seeburg PH (1994) Regional and developmental heterogeneity in splicing of the rat brain NMDAR1 mRNA. *J Neurosci* **14:**3180–3194.

Luo J, Wang Y, Yasuda RP, Dunah AW, and Wolfe BB (1997) The majority of *N*-methyl-D-aspartate receptor complexes in adult rat cerebral cortex contain at least three different subunits (NR1/NR2A/NR2B). *Mol Pharmacol* **51:**79–86.

Matsuda K, Kamiya, Y Matsuda S, and Yuzaki M (2002) Cloning and characterization of a novel NMDA receptor subunit NR3B: a dominant subunit that reduces calcium permeability. *Mol Brain Res* **100:**43–52.

McBain CJ and Mayer ML (1994) *N*-Methyl-D-aspartic acid receptor structure and function. *Physiol Rev* **74:**723–760.

Monyer H, Burnashev N, Laurie DJ, Sakmann B, and Seeburg PH (1994) Developmental and regional expression in the rat brain and functional properties of four NMDA receptors. *Neuron* **12:**529–540.

Monyer H, Sprengel R, Schoepfer R, Herb A, Higuchi M, Lomeli H, Burnashev N, Sakmann B, and Seeburg PH (1992) Heteromeric NMDA receptors: molecular and functional distinction of subtypes. *Science (Wash DC)* 256(5060):1217–1221.

Nishi M, Hinds H, Lu HP, Kawata M, and Hayashi Y (2001) Motoneuron-specific expression of NR3B, a novel NMDA-type glutamate receptor subunit that works in a dominant-negative manner. *J Neurosci* **21:**RC185.

Pérez-Otaño I, Schulteis CT, Contractor A, Lipton SA, Trimmer JS, Sucher NJ, and Heinemann SF (2001) Assembly with the NR1 subunit is required for surface expression of NR3A-containing NMDA receptors. *J Neurosci* **21:**1228–1237.

Prybylowski KL and Wolfe BB (2000) Developmental differences in alternative splicing of the NR1 protein in rat cortex and cerebellum. *Brain Res Dev Brain Res* **123:**143–150.

Rumbaugh G and Vicini S (1999) Distinct synaptic and extrasynaptic NMDA receptors in developing cerebellar granule neurons. *J Neurosci* **19:**10603–10610.

Stocca G and Vicini S (1998) Increased contribution of NR2A subunit to synaptic NMDA receptors in developing rat cortical neurons. *J Physiol (Lond)* **507:**13–24.

Sucher NJ, Akbarian S, Chi CL, Leclerc CL, Awobuluyi M, Deitcher DL, Wu MK, Yuan JP, Jones EG, and Lipton SA (1995) Developmental and regional expression

pattern of a novel NMDA receptor-like subunit (NMDAR-L) in the rodent brain. *J Neurosci* **15:**6509–6520.

Sun L, Margolis FL, Shipley MT, and Lidow MS (1998) Identification of a long variant of mRNA encoding the NR3 subunit of the NMDA receptor: its regional distribution and developmental expression in the rat brain. *FEBS Lett* **441:**392–396.

Sun L, Shipley MT, and Lidow MS (2000) Expression of NR1, NR2A-D and NR3 subunits of the NMDA receptor in the cerebral cortex and olfactory bulb of adult rat. *Synapse* **35:**212–221.

Tovar KR, Sprouffske K, and Westbrook GL (2000) Fast NMDA receptor-mediated synaptic currents in neurons from mice lacking the epsilon2 (NR2B) subunit. *J Neurophysiol* **83:**616–620.

Wang YH, Bosy TZ, Yasuda RP, Grayson DR, Vicini S, Pizzorusso T, and Wolfe BB (1995) Characterization of NMDA receptor subunit-specific antibodies: distribution of NR2A and NR2B receptor subunits in rat brain and ontogenic profile in the cerebellum. *J Neurochem* **65:**176–183.

Watanabe M, Inoue Y, Sakimura K, and Mishina M (1992) Developmental changes in distribution of NMDA receptor channel subunit mRNAs. *Neuroreport* **3:**1138–1140.

Williams K, Russell SL, Shen YM, and Molinoff PB (1993) Developmental switch in the expression of NMDA receptors occurs in vivo and in vitro. *Neuron* **10:**267–278.

Zhong J, Carrozza DP, Williams K, Pritchett DB, and Molinoff PB (1995) Expression of mRNAs encoding subunits of the NMDA receptor in developing rat brain. *J Neurochem* **64:**531–539.

Zukin RS and Bennett MV (1995) Alternatively spliced isoforms of the NMDARI receptor subunit [published erratum appears in *Trends Neurosci* (1995) **18:**441]. *Trends Neurosci* **18:**306–313.

Address correspondence to: Robert Yasuda, Department of Pharmacology, Med-Dent 401, Georgetown University School of Medicine, 3900 Reservoir Road NW, Washington, DC 20007. E-mail: yasudar@georgetown.edu